Hindawi
Journal of Spectroscopy
Volume 2019, Article ID 2853989, 5 pages
https://doi.org/10.1155/2019/2853989

Research Article

Effect of Adsorption Characteristics of Rhodamine 6G Dye Solution in Fe_3O_4 Magnetic Nanoparticles on Fluorescence Quantum Yield

Suwaphit Phoemphoonthanyakit,[1] Panpailin Seeharaj,[2] Pattareeya Damrongsak,[1] and Kitsakorn Locharoenrat[1]

[1]*Biomedical Physics Research Unit, Department of Physics, Faculty of Science, King Mongkut's Institute of Technology Ladkrabang, Bangkok 10520, Thailand*
[2]*Department of Chemistry, Faculty of Science, King Mongkut's Institute of Technology Ladkrabang, Bangkok 10520, Thailand*

Correspondence should be addressed to Kitsakorn Locharoenrat; kitsakorn.lo@kmitl.ac.th

Received 7 March 2019; Accepted 25 June 2019; Published 3 July 2019

Academic Editor: K.S.V. Krishna Rao

Copyright © 2019 Suwaphit Phoemphoonthanyakit et al. This is an open access article distributed under the Creative Commons Attribution License, which permits unrestricted use, distribution, and reproduction in any medium, provided the original work is properly cited.

In this work, the use of Fe_3O_4 magnetic nanoparticles in the adsorption of rhodamine 6G solution was evaluated via absorbance and fluorescence spectroscopy using the UV-Vis spectrometer. The adsorption mechanism of rhodamine 6G on Fe_3O_4 was determined with respect to the adsorbent dosage (2.5–10 mg/L) and treatment time (0–150 min). The experimental data revealed that the fluorescence quantum yield of rhodamine 6G was inversely proportional to the percentage of dye removal. The highest efficiency of dye removal was obtained at 10 mg/L Fe_3O_4, and the adsorption capacity was about 150 mg/g, together with a reduced treatment time of 30 min, owing to active adsorption of Fe_3O_4. We believe that our study makes a significant contribution to the literature because Fe_3O_4 magnetic nanoparticles were found to be able to quench rhodamine 6G dye molecules, which will aid in eliminating toxic and hazardous pollutants from dye wastewater, which are otherwise detrimental to the environment and human health.

1. Introduction

Nowadays, the textile industry, being the highest user of dyes for fiber coloration, is faced with the challenge of disposal of dye wastewater worldwide. Effluents derived from many manufacturing units are sometimes discharged into water resources without any treatment, partly due to economic and technical restrictions. Because most dyes are stable against oxidizing agents and sunlight, nonremoval of color from dye wastewater is becoming one of the main water pollutants. They cause severe environmental hazards, not only affecting the aesthetic merit but also decreasing the penetration of light, and it can even prove to be carcinogenic for humans. As a result, various physical, chemical, and biological techniques have been developed to eliminate dissolved inorganic/organic compounds by converting them into harmless end products. Among these treatment approaches, physical adsorption on activated carbon is a very practical one to produce effluents composing low level of these compounds [1–3]. However, the use of alternative substitutes to eliminate such dyes from other materials like nanomaterials has emerged as they are able to treat a large amount of dye wastewater and are not time-consuming and produce a low amount of contaminants. In recent years, magnetic nanoparticles have gained considerable interest with regard to environmental concerns. Among them, Fe_3O_4 is considered as a good candidate capable of removal of original dyes [4]; however, there is no empirical study on the relationship between the adsorption process of dyes and fluorescence quantum yield. Fe_3O_4 nanoparticles have been proved to be biocompatible with low-toxicity and are applicable for a variety of biomedical researches. For instance,

they are commonly used as a contract agent, therapeutic agent, and sensing probe for magnetic resonance imaging, hyperthermia therapy, and targeted-drug delivery, respectively [5]. However, although there are many common cationic rhodamine family dyes used in the textile industry, only a few studies have been focused on adsorption behaviors of rhodamine 6G. Therefore, in this study, we select rhodamine 6G as a dye model to elucidate the interaction mechanism between Fe_3O_4 magnetic nanoparticles and rhodamine 6G dye. Based on dosages of Fe_3O_4 magnetic nanoparticles, it is possible to observe both amplification and quenching of fluorescence of dye molecules.

2. Materials and Methods

Iron-(II,III) oxide or Fe_3O_4 with particle sizes in the range of 50–100 nm and cationic dye rhodamine 6G were purchased from Sigma-Aldrich, USA. The dye powder was first dissolved in deionized water for use as a stock solution. The stock solution was, then, diluted in two proportions. The first portion was used to acquire a calibration curve as $y = 79289x - 0.0032$, where y and x represent the absorbance peak and rhodamine 6G concentration, respectively, as shown in Figure 1.

The second portion was used further as adsorbate. Next, the adsorption experiments were performed by mixing 1 mL dye solution of fixed concentration (3 μM rhodamine 6G) and 1 mL adsorbent of known quantity (2.5–10 mg/L Fe_3O_4) under a sonicator at the room temperature of 26°C and pH 7.0. The treatment time was varied from 0 to 150 min. At every 30 min time interval, the mix solution was studied under the UV-Vis spectrometer by measuring the absorbance at wavelength of 525 nm and fluorescence at wavelength 555 nm. More details of the optical setup were explained in [6]. Fluorescence quantum yield, efficient removal of dye, and amount of dye adsorbed on adsorbent were calculated using the following equations:

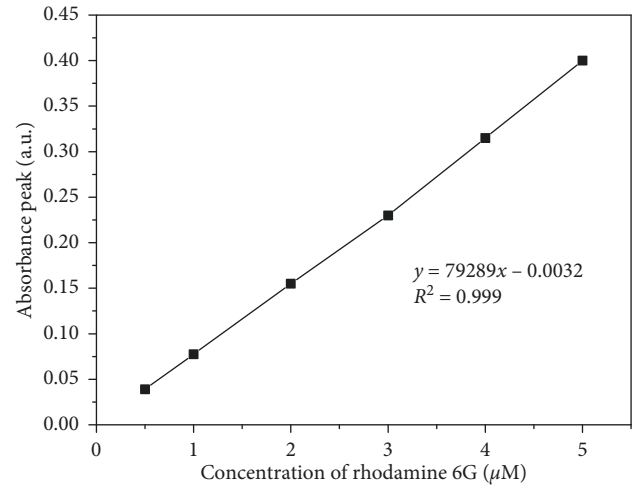

Figure 1: Calibration curve of rhodamine 6G dye concentration determination.

Fluorescence quantum yield (Q) was calculated by [6]

$$Q = Q_{\mathrm{REF}} \cdot \frac{I}{A} \cdot \frac{A_{\mathrm{REF}}}{I_{\mathrm{REF}}} \cdot \frac{n^2}{n_{\mathrm{REF}}^2}, \quad (1)$$

where I and A are the integrated fluorescence intensity and absorbance peak, respectively; n is the refractive index of the solvent; and subscript REF is the reference fluorophore. The dye concentration was calculated from the calibration curve.

Efficiency of dye concentration removal was calculated as follows:

$$\%\ \text{dye removal} = \frac{\text{initial concentration of dye} - \text{equilibrium concentration of dye}}{\text{initial concentration of dye}} \times 100. \quad (2)$$

Amount of dye adsorbed on the adsorbent at equilibrium state was calculated as follows:

$$\text{adsorption capacity} = \frac{\text{initial concentration of dye} - \text{equilibrium concentration of dye}}{\text{mass of adsorbent}} \times \text{volume of solution}. \quad (3)$$

3. Results and Discussion

Adsorbent dosage is an imperative factor in the determination of its adsorption capacity on an adsorbate. To verify the effect of the adsorbent dosage on rhodamine 6G adsorption, adsorption experiments were performed by mixing the Fe_3O_4 dosage (2.5, 5.0, 7.5, and 10.0 mg/L) in a solution form, for certain amount of rhodamine 6G of 3.0 μM at a room temperature of 26°C and pH 7.0 and for time intervals from 0 to 150 min. The absorption and fluorescence intensities of the mixed solution are displayed in Figures 2 and 3, respectively, and the absorbance peak and integrated fluorescence intensity of the solution are shown in Figures 4 and 5, respectively. The absorption and fluorescence intensities of Fe_3O_4 mixed with rhodamine 6G are found to be remarkably lower than those of rhodamine 6G alone. They all tend to decrease as dosages of Fe_3O_4 magnetic nanoparticles increase, owing to the following reasons. Since a surface-to-volume ratio of Fe_3O_4 is high, it intensely adsorbs rhodamine 6G. A reduction in the fluorescence intensity will thus occur due to the inner filter effect [7]. The fluorescence intensity reduces not only due to the strong adsorption capacity of Fe_3O_4 but also due to the fluorescence energy resonance transfer of rhodamine 6G by the Fe_3O_4

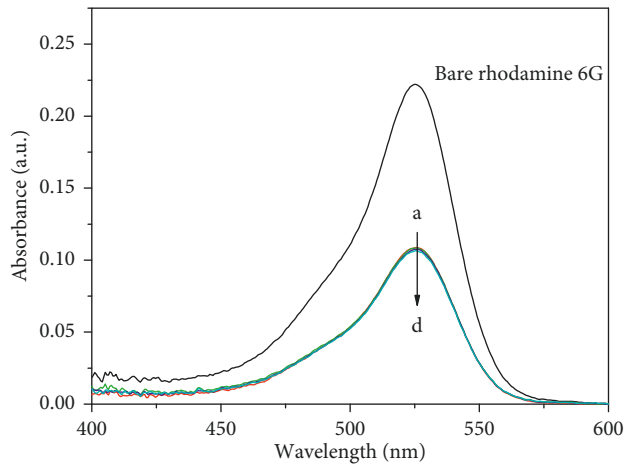

Figure 2: Absorbance spectra of 3.0 μM rhodamine 6G mixed with four different dosages of Fe_3O_4 magnetic nanoparticles. The treatment time is 0 min, as a representative sample. a, b, c, and d represent Fe_3O_4 magnetic nanoparticles dosages of 2.5, 5.0, 7.5, and 10.0 mg/L, respectively. Absorbance peak exists at 525 nm.

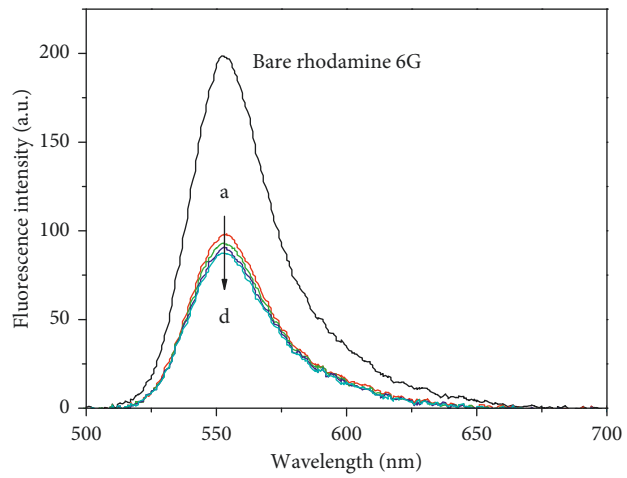

Figure 3: Fluorescence spectra of 3.0 μM rhodamine 6G mixed with four different dosages of Fe_3O_4 magnetic nanoparticles. The treatment time is 0 min as a representative sample. a, b, c, and d represent Fe_3O_4 magnetic nanoparticles dosages of 2.5, 5.0, 7.5, and 10.0 mg/L, respectively. Peak fluorescence exists at 555 nm.

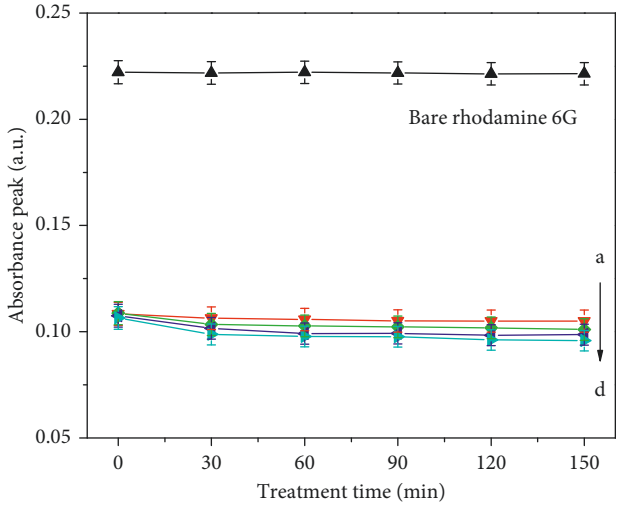

Figure 4: Absorbance peak of 3.0 μM rhodamine 6G mixed with four different dosages of Fe_3O_4 nanoparticles under six different treatment times. a, b, c, and d represent Fe_3O_4 magnetic nanoparticles dosages of 2.5, 5.0, 7.5, and 10.0 mg/L, respectively.

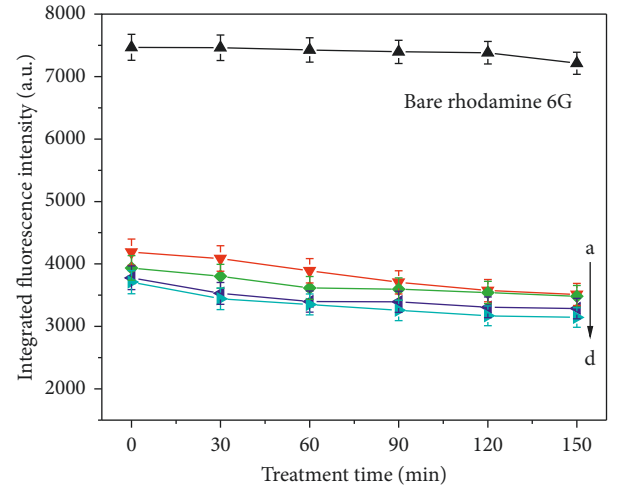

Figure 5: Integrated fluorescence intensity of 3.0 μM rhodamine 6G mixed with four different dosages of Fe_3O_4 magnetic nanoparticles under six different treatment times. a, b, c, and d represent Fe_3O_4 magnetic nanoparticles dosages of 2.5, 5.0, 7.5, and 10.0 mg/L, respectively.

nanoparticles. It is a nonradiative energy transfer from an excited donor fluorophore to an acceptor though nonradiative dipole-dipole coupling [8–10]. Hence, it is possible to quench the rhodamine 6G dye molecule by Fe_3O_4.

A reduction of both absorption and fluorescence intensities further results in a significant decrease in the fluorescence quantum yield, calculated using equation (1) and as shown in Figure 6. The fluorescence quantum yield is in the range of 0.81–0.88. In Figure 7, the fluorescence quantum yield is plotted with respect to the dye removal calculated using equation (2). The fluorescence quantum yield is inversely proportional to dye removal. That is, with the increase in dye removal, the fluorescence quantum yield gradually decreases. The relationship is linear, which further confirms that Fe_3O_4 magnetic nanoparticles are an efficient fluorescence quencher for rhodamine 6G. The observed fluorescence mechanism of rhodamine 6G under the influence of Fe_3O_4 magnetic nanoparticles possibly involves fluorescence resonance energy transfer between the dye molecule and Fe_3O_4 magnetic nanoparticles.

The effect of Fe_3O_4 dosage on rhodamine 6G concentration removal shows a small change, as displayed in Figure 8; however, the adsorption capacity of Fe_3O_4 calculated using equation (3) shows a considerable change, as exhibited in Figure 9. The adsorption capacity is in the range of 150–600 mg/g. It is seen that the treatment time profile of rhodamine 6G uptake is a smooth and continuous curve leading to a saturation stage, indicating the available

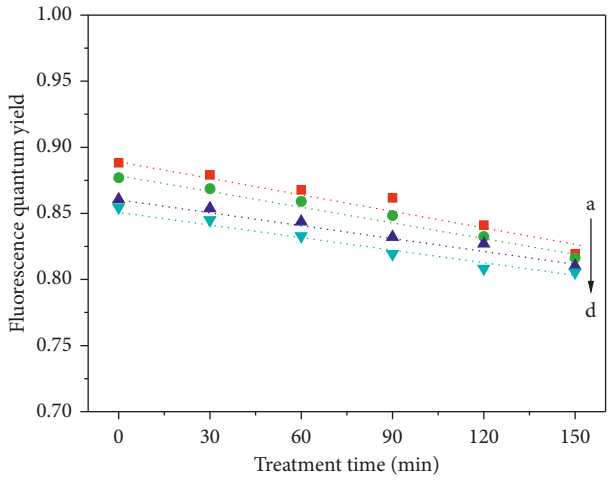

Figure 6: Percentage of fluorescence quantum yield of 3.0 μM rhodamine 6G mixed with four different dosages of Fe_3O_4 magnetic nanoparticles under six different treatment times. a, b, c, and d represent Fe_3O_4 magnetic nanoparticles dosages of 2.5, 5.0, 7.5, and 10.0 mg/L, respectively. Dashed lines are for guide to the eyes.

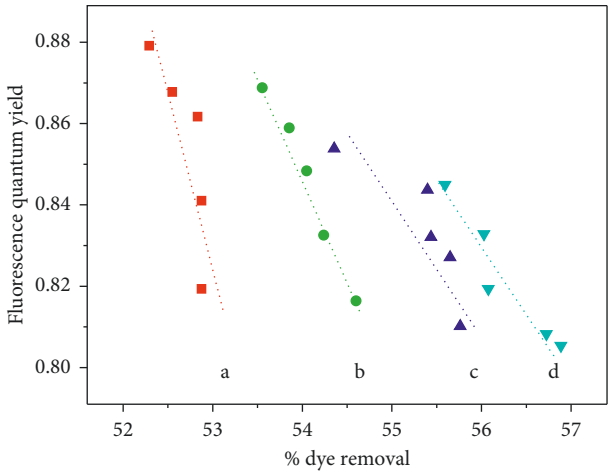

Figure 7: Relationship between fluorescence quantum yield and dye removal of 3.0 μM rhodamine 6G mixed with four different dosages of Fe_3O_4 magnetic nanoparticles under six different treatment times. a, b, c, and d represent Fe_3O_4 magnetic nanoparticles dosages of 2.5, 5.0, 7.5, and 10.0 mg/L, respectively. Dashed lines are for guide to the eyes.

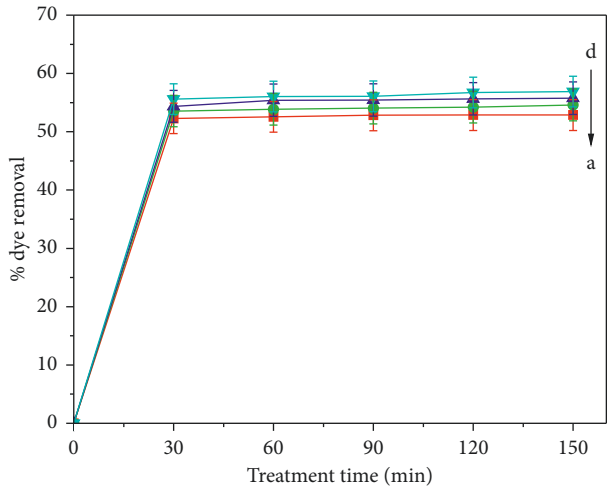

Figure 8: Percentage of dye removal of 3.0 μM rhodamine 6G mixed with four different dosages of Fe_3O_4 magnetic nanoparticles under six different treatment times. a, b, c, and d represent Fe_3O_4 magnetic nanoparticles dosages of 2.5, 5.0, 7.5, and 10.0 mg/L, respectively.

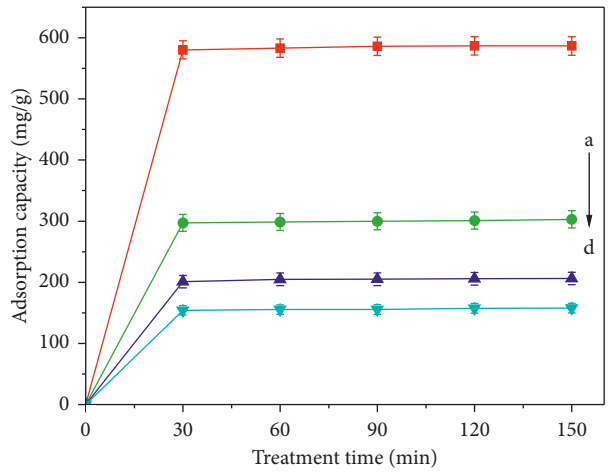

Figure 9: Adsorption capacity of 3.0 μM rhodamine 6G mixed with four different dosages of Fe_3O_4 magnetic nanoparticles under six different treatment times. a, b, c, and d represent Fe_3O_4 magnetic nanoparticles dosages of 2.5, 5.0, 7.5, and 10.0 mg/L, respectively.

monolayer coverage of rhodamine 6G on the surface of Fe_3O_4.

In all cases, it is clearly seen that the adsorption of rhodamine 6G is rapid at the first treatment time of 30 min because the mass transfer driving force is large. Adsorption of rhodamine 6G remains constant after reaching an equilibrium state because rhodamine 6G reaches a boundary layer and then possibly diffuses into the tiny pores of Fe_3O_4. Furthermore, the equilibrium time is shorter at a higher Fe_3O_4 dosage. This is because, as the Fe_3O_4 dosage increases, the surface area of Fe_3O_4 will increase, leading to higher availability of active adsorbent sites to adsorb rhodamine 6G from aqueous solution. Furthermore, at each equilibrium time, it is found that the percentage of rhodamine 6G concentration removal tends to increase from 52 to 57% when the Fe_3O_4 dosage is increased from 2.5 to 10.0 mg/L, respectively. It is believed that the removal percentage would not go beyond 60% even when more than 10 mg/L of Fe_3O_4 is added. These results are in good agreement with those in [4]. Thus, the highest efficiency of dye removal is achieved at 10 mg/L Fe_3O_4, whereas the corresponding adsorption capacity is about 150 mg/g in this study. This value is still higher in comparison with the results reported over the last ten years [11, 12] in other studies on the adsorption of different dyes on different adsorbents, except for [13]. The best treatment time in our adsorption process is 30 min, involving low operation cost that is very important for

industry-scale application of an adsorbent. Since rhodamine 6G concentration removal cannot reach 100% similar to [4], partly due to the aggregation of Fe_3O_4 surface area available to rhodamine 6G and consequently a reduction in the diffusion path length, application of UV light irradiation is suggested to be added in the present process in order to further improve the adsorption capacity. It is expected that the dye removal might go beyond 60% in that case and a comparative study will be presented in the future.

4. Conclusions

The effectiveness of Fe_3O_4 magnetic nanoparticles as an adsorbent for the elimination of rhodamine 6G dye solution was investigated in this study, by using a UV-Vis spectrometer. Further, amplification and quenching of fluorescence of dye molecules were observed with respect to the dosage of Fe_3O_4 nanoparticles. Upon the addition of Fe_3O_4 in rhodamine 6G solution, the absorption and fluorescence intensities were significantly reduced due to the adsorption of rhodamine 6G molecules on the surface of Fe_3O_4 and the quenching of rhodamine 6G as a fluorophore. The fluorescence quantum yield of rhodamine 6G was therefore decreased, conforming to an increase in dye removal. The highest efficiency of dye removal was achieved at 10 mg/L Fe_3O_4, whereas the corresponding adsorption capacity was approximately 150 mg/g at a shortened treatment time of 30 min. It is expected that Fe_3O_4 magnetic nanoparticles will be applied as an adsorbent for elimination of a variety of toxic and hazardous pollutants from dye wastewater because the magnetic nanoparticles have a high surface-to-volume ratio and appropriate pore size for adsorption of dye molecules.

Data Availability

The data used to support the findings of this study are included within the article.

Conflicts of Interest

The authors declare that there are no conflicts of interest regarding this study.

Acknowledgments

This research was funded by the King Mongkut's Institute of Technology, Ladkrabang, Bangkok 10520, Thailand.

References

[1] L. Ding, B. Zou, W. Gao et al., "Adsorption of rhodamine-B from aqueous solution using treated rice husk-based activated carbon," *Colloids and Surfaces A: Physicochemical and Engineering Aspects*, vol. 446, no. 5, pp. 1–7, 2014.

[2] Z. Chennouf-Abdellatif, B. Cheknane, F. Zermane, E. M. Gaigneaux, O. Mohammedi, and N. Bouchenafa-Saib, "Equilibrium and kinetic studies of methyl orange and rhodamine B adsorption onto prepared activated carbon based on synthetic and agricultural wastes," *Desalination and Water Treatment*, vol. 67, pp. 284–291, 2017.

[3] M. Danish, T. Ahmad, R. Hashim et al., "Comparison of surface properties of wood biomass activated carbons and their application against rhodamine B and methylene blue dye," *Surfaces and Interfaces*, vol. 11, pp. 1–13, 2018.

[4] A. Khorshid and M. Hajnajafi, "Degradation of rhodamine 6G in aqueous solution by using Au/Fe_3O_4 core/shell nanoparticles," *Journal of Applied Chemistry*, vol. 13, no. 47, pp. 21–34, 2018.

[5] N. T. K. Thanh, *Clinical Applications of Magnetic Nanoparticles*, CRC Press, Boca Raton, FL, USA, 2018.

[6] E. Rammarat, K. Locharoenrat, W. Yindeesuk, and P. Damrongsak, "Studies of concentration dependence of the fluorescent quantum yield from rhodamine 6G and Au–Pd core–shell nanorods, using a response surface methodology," *Ukrainian Journal of Physical Optics*, vol. 18, no. 3, pp. 179–186, 2017.

[7] A. V. Fonin, A. I. Sulatskaya, I. M. Kuznetsova, and K. K. Turiverov, "Fluorescence of dyes in solutions with high absorbance. Inner filter effect correction," *PLoS One*, vol. 9, no. 7, Article ID e103878, 2014.

[8] P.-J. J. Huang and J. Liu, "Molecular beacon lighting up on graphene oxide," *Analytical Chemistry*, vol. 84, no. 9, pp. 4192–4198, 2012.

[9] M. Ujihara, N. M. Dang, and T. Imae, "Fluorescence quenching of uranine on confeito-like Au nanoparticles," *Journal of Nanoscience and Nanotechnology*, vol. 14, no. 7, pp. 4906–4910, 2014.

[10] B. Gilbert, J. E. Katz, N. Huse et al., "Ultrafast electron and energy transfer in dye-sensitized iron oxide and oxyhydroxide nanoparticles," *Physical Chemistry Chemical Physics*, vol. 15, no. 40, pp. 17303–17313, 2013.

[11] B. Uçar, A. Güvenç, and Ü. Mehmetoglu, "Use of aluminium hydroxide sludge as adsorbents for the removal of reactive dyes: equilibrium, thermodynamic, and kinetic studies," *Hydrology Current Research*, vol. 2, no. 2, article 1000112, 2011.

[12] A. Azizi, M. A. Moghaddam, and M. Arami, "Removal of a reactive dye using ash of pulp and paper sludge," *Journal of Residuals Science and Technology*, vol. 9, pp. 159–168, 2012.

[13] S. C. R. Santos and R. A. R. Boaventura, "Treatment of a simulated textile wastewater in a sequencing batch reactor (SBR) with addition of a low-cost adsorbent," *Journal of Hazardous Materials*, vol. 291, pp. 74–82, 2015.

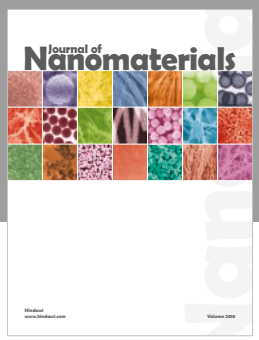

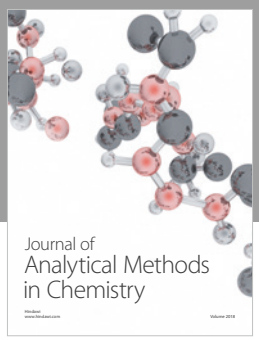

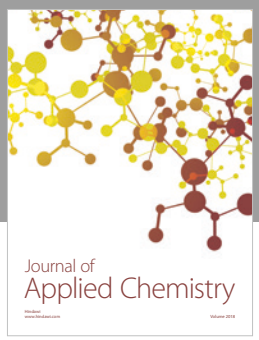

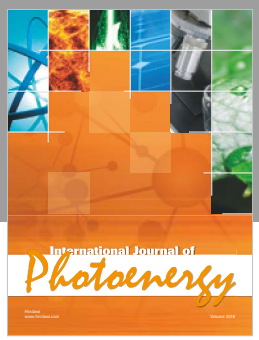

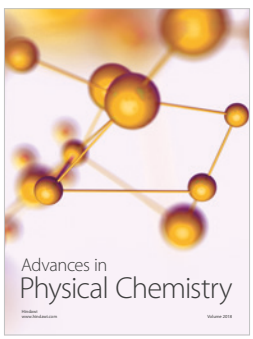

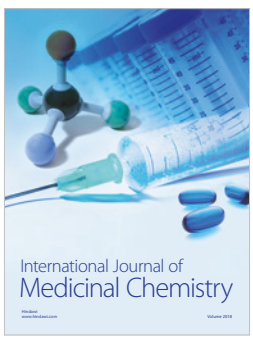

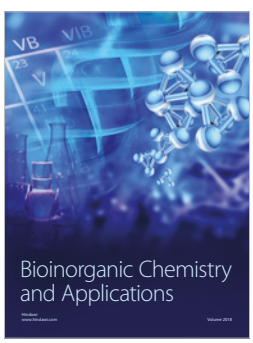

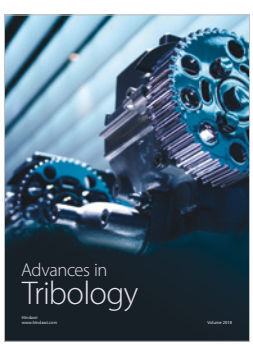

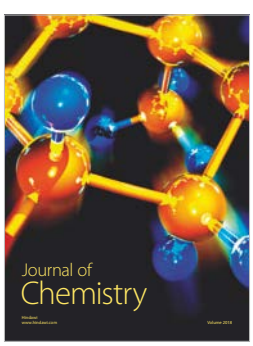

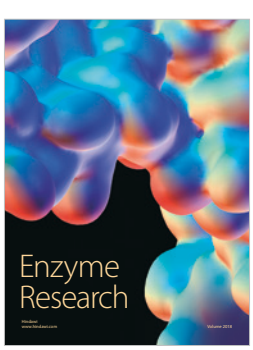

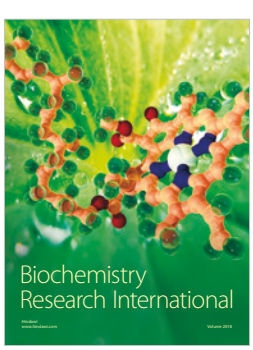

Hindawi

Submit your manuscripts at
www.hindawi.com